

# High-resolution electron microscope study of the ordered lead–calcium titanate ceramics

FEI FANG, XIAOWEN ZHANG

*Department of Materials Science and Engineering, Tsinghua University, Beijing 100084, People's Republic of China*

High-resolution electron microscopy (HREM) has been used to demonstrate the structural characteristics of ordered  $(\text{Pb}_{0.5}\text{Ca}_{0.5})\text{TiO}_3$ . The fine structure of both ordered and disordered domains was exposed in lattice level. It was shown that there are  $1/2\{111\}$ ,  $1/2\{110\}$  and  $1/2\{111\}$  ordering coexisted in  $(\text{Pb}_{0.5}\text{Ca}_{0.5})\text{TiO}_3$  and all of them are chemical ordering due to the layers of  $\text{Pb}^{2+}$  and  $\text{Ca}^{2+}$  cations align alternatively along different directions. For  $1/2\{111\}$  chemical ordering, a special type of boundary defined as "vernier boundary" was introduced.

## 1. Introduction

Relaxors with lead–base complex perovskite structure  $\text{Pb}(\text{B}'\text{B}'')\text{O}_3$  possess highly desirable dielectric and electrostrictive properties that have great potential for use in many applications [1–3]. It has been pointed out that the dielectric properties including diffuse phase transition and frequency dependent ferroelectric behaviour are related to the order–disorder arrangement of two different cations on the B-site [4]. It has also been demonstrated that the difference in ion charges and ion size between  $\text{B}'$  and  $\text{B}''$  have great influence on B-site cation ordering [5]. So far, no superstructure has been found for compounds with the same ion charge on the B-site, such as lead zirconate titanate ceramics  $(\text{Pb}(\text{ZrTi})\text{O}_3)$ . Comparatively less work has been done on the order–disorder transition of  $(\text{A}'\text{A}'')\text{BO}_3$  perovskite compounds. Randall *et al.* [6] once reported the existence of  $\{h + 1/2, k + 1/2, 0\}$  superlattice in  $(\text{PbLa})(\text{ZrTi})\text{O}_3$  and recently we [7] confirmed that this type of superstructure originated from the ordering of lead cations ( $\text{Pb}^{2+}$ ), lanthanum cations and lead vacancies ( $\text{La}^{3+} + \text{V}_{\text{Pb}}$ ) on the A-site resulting in a body-centred pseudo-cubic superstructure. It's easy to understand A-site cation ordering in  $(\text{PbLa})(\text{ZrTi})\text{O}_3$  because ion charges of  $\text{La}^{3+}$  and  $\text{Pb}^{2+}$  are not the same. But for the same ion charges on A-site cations, whether  $\text{A}'$  and  $\text{A}''$  can be ordered remains unknown until King and co-workers [8] reported the existence of  $1/2\{110\}$ ,  $1/2\{100\}$  and  $1/2\{111\}$  superlattice in  $(\text{PbCa})\text{TiO}_3$ . They postulated that  $1/2\{111\}$  is the result of chemical ordering of  $\text{Pb}^{2+}$  and  $\text{Ca}^{2+}$  while the other two are the results of electrical ordering due to the atomic shuffles. Gu *et al.* [9] demonstrated the probability of various kinds of chemical ordering in perovskite  $(\text{A}'\text{A}'')\text{BO}_3$  compounds with the ion charge of  $\text{A}'$  equal to that of  $\text{A}''$ . Based on the atomic configuration probability wave theory, it has been pointed out that the second and third neighbour interaction have an important effect on the ordering of A-site cations with

the same ionic charges and concluded that there are seven kinds of chemical ordering including  $1/2\{100\}$ ,  $1/2\{110\}$ ,  $1/2\{111\}$  by taking them into consideration (as shown in Fig. 1). In this paper, the fine superstructure in lattice level was exposed in detail by high-resolution transmission electron microscopy (HREM) to demonstrate that not only the  $1/2\{111\}$ , but also the  $1/2\{110\}$  and  $1/2\{100\}$  superstructures are the results of chemical ordering.

## 2. Experimental procedure

In order to reduce the energy for ordering, the composition of  $(\text{Pb}_{1-x}\text{Ca}_x)\text{TiO}_3$  with  $x = 0.5$  was suggested both theoretically and practically [8]. Starting materials were reagent-grade powders of  $\text{Pb}_3\text{O}_4$  (99.5%),  $\text{CaCO}_3$  (99%) and  $\text{TiO}_2$  (98%). They were properly weighed and mixed by ball milling in alcohol and calcined in a closed alumina crucible at  $800^\circ\text{C}$  for 1 h. After calcining, the powders were remilled, dried and sieved, then pressed into discs 1.2 mm thick and 10 mm in diameter and sintered at  $1150^\circ\text{C}$  for 2 h in a closed aluminium crucible.

The HREM sample was prepared by grinding a piece of bulk sample into fine powder in an agate mortar with alcohol, then dropping it onto a copper grid with a carbon micro-sieve. The observations were performed on a top-entry H9000 NAR high-resolution transmission electron microscope with a double tilt stage, operating at 300 kV.

## 3. Experimental results

Upon chemical ordering, the structure of the unit cell will be changed, resulting in modified diffraction patterns and extra lattice fringes. In order to expose the distinction between ordered and disordered regions by HREM, the sample must be rotated to the proper orientation, in which both ordered and disordered lattice fringes can be resolved and distinguished.

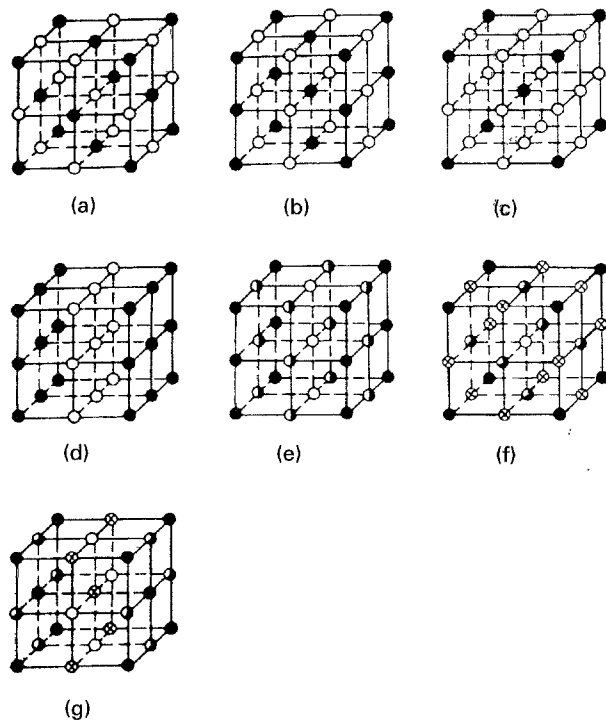


Figure 1 Seven kinds of ordered structure theoretically existed in complex perovskite materials (a) the superlattice in the  $[111]$  direction, (b) the superlattice in the  $[110]$  direction, (c) the superlattice in the  $\langle 110 \rangle$  direction, (d) the superlattice in the  $[100]$  direction, (e) the superlattice in the  $[100]$ ,  $[010]$  and  $[110]$  directions, (f) the superlattice in the  $\langle 100 \rangle$ ,  $\langle 110 \rangle$  and  $[110]$  directions and (g) the superlattice in the  $[100]$ ,  $[110]$  and  $[111]$  directions.

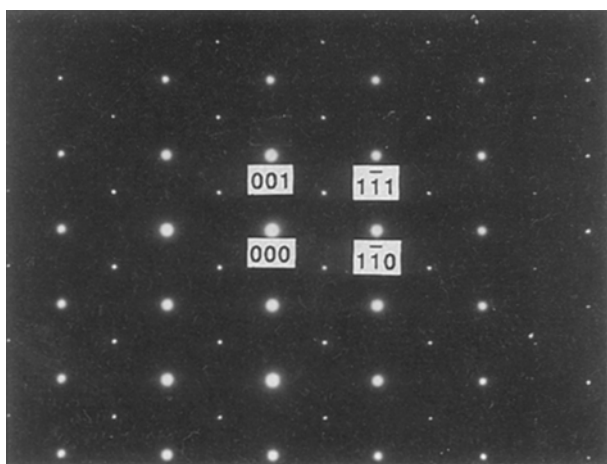


Figure 2 A  $[110]$  zone axis selected electron diffraction pattern showing  $1/2\{111\}$  superlattice reflections.

Fig. 2 is a  $[110]$  zone axis selected area electron diffraction (SAD) pattern showing  $1/2\{111\}$  superlattice reflections. Indexing of it reveals that the sample belongs to pseudo-cubic structure with the unit parameter equal to 0.389 nm, which is also consistent with our previous X-ray diffraction results. The corresponding  $[110]$  zone axis high resolution electron micrograph is shown in Fig. 3(a). Fig. 3(b) represents the projection image of A-site cations ( $\text{Pb}^{2+}$ ,  $\text{Ca}^{2+}$ ) on the  $(110)$  plane showing the configuration difference between the disordered and  $1/2\{111\}$ -type ordered structure (see Fig. 1(a)), which is fully consistent

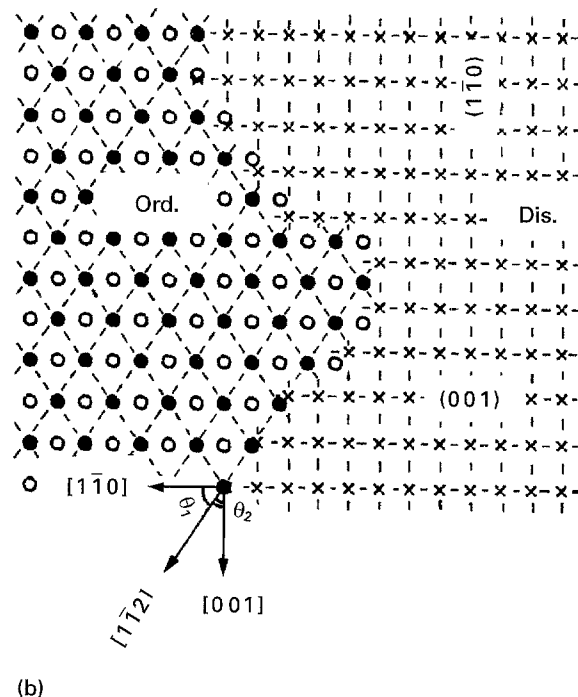
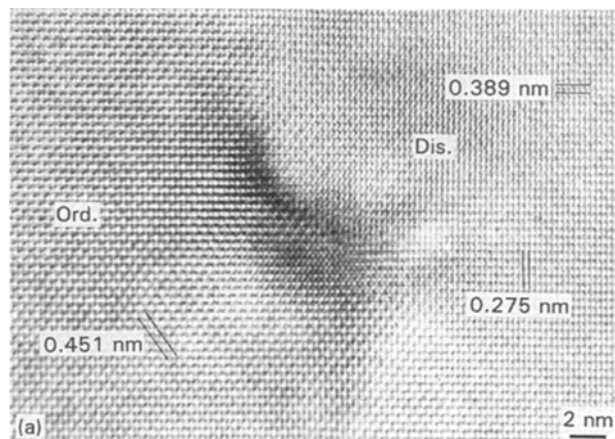


Figure 3 (a) A  $[110]$  zone axis high resolution electron micrograph with both ordered and disordered structure regions. (b) The projection image of  $\text{Pb}^{2+}$  and  $\text{Ca}^{2+}$  cations on the  $(110)$  plane showing the configuration difference between the disordered and  $1/2\{111\}$ -type ordered structure.

with the HREM image as shown in Fig. 3(a). When  $\text{Pb}^{2+}$  and  $\text{Ca}^{2+}$  cations are in disordered state (designated as "Dis."),  $(001)$  planes with spacing of 0.389 nm array perpendicular to  $(1\bar{1}0)$  planes with spacing of 0.275 nm. However, when they align alternately along both  $[1\bar{1}0]$  and  $[001]$  in the projection of  $(110)$  plane, the unit cell will be doubled and superlattice fringes of  $1/2(\bar{1}11)$  appear with spacing of 0.451 nm and  $\theta_1 = 54.3^\circ$  or  $\theta_2 = 35.7^\circ$ , which is quite close to the theoretical angle between  $(\bar{1}11)$  and  $(001)$  ( $54.73^\circ$ ) or the angle between  $(\bar{1}11)$  and  $(1\bar{1}0)$  ( $35.27^\circ$ ) in ideal cubic structure. However, there is slight distortion for ordered superstructure and thus a special kind of boundary will be caused, which will be discussed later.

Fig. 4 is an electron diffraction pattern for the  $[001]$  zone axis showing  $1/2\{110\}$  superlattice reflections. Fig. 5(a) is the corresponding HREM image to show both the disordered and the  $1/2\{110\}$  superstructure

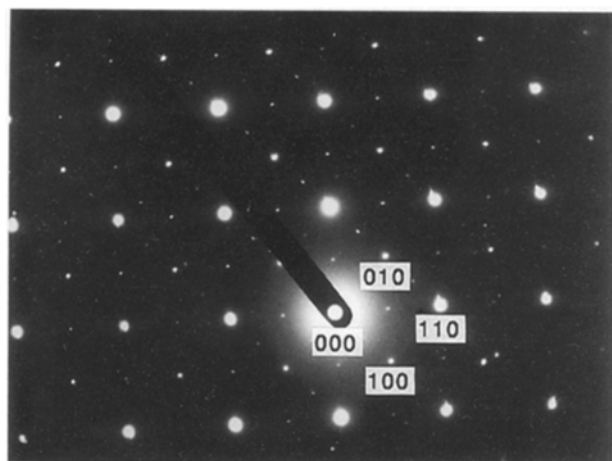


Figure 4 A [001] zone axis electron diffraction pattern showing  $1/2\{110\}$  superlattice reflections.

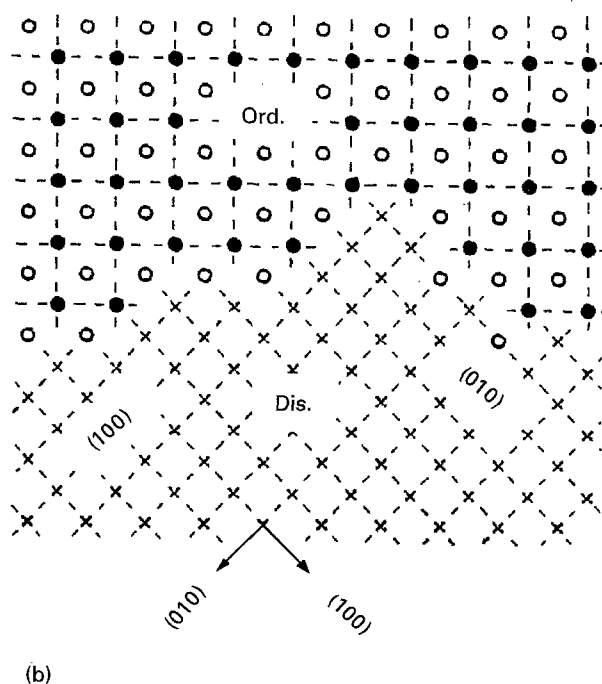
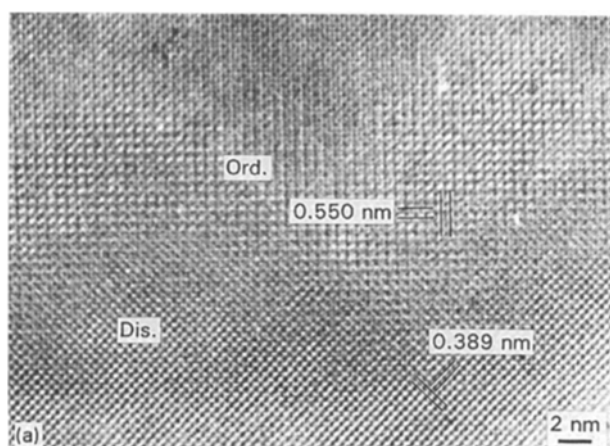


Figure 5 (a) A [001] zone axis HREM image with both  $1/2\{110\}$  ordered and disordered structure regions. (b) The projection image of  $\text{Pb}^{2+}$  and  $\text{Ca}^{2+}$  cations on (001) plane for both disordered and  $1/2\{110\}$  ordered structure.

region in the same micrograph. There are apparently two different sets of lattice fringes with an angle of  $45^\circ$  between them. The narrower refer to  $\{100\}$  planes with spacing of 0.389 nm. The wider are  $1/2\{110\}$  superlattice with spacing of 0.550 nm. Fig. 5(b) is the projection image of A-site cations on (001) plane for both disordered and  $1/2\{110\}$  ordered structure, which is consistent with the corresponding [110] zone axis HREM image. Both ordered and disordered regions can form the narrower lattice fringes. But only when the layers of  $\text{Pb}^{2+}$  and  $\text{Ca}^{2+}$  cations align alternately along [110] (see Fig. 1(b)) can the wider lattice fringes be formed. So the regions with only narrower lattice fringes of perpendicular (100) and (010) planes are referred to disordered regions (designated as “Dis.”), while those with wider lattice fringes are ordered regions (indicated as “Ord.”).

Fig. 6 is another [001] zone axis selected electron diffraction pattern showing  $1/2\{100\}$  superlattice reflections. The high resolution electron micrograph with the same crystallographic projection is shown in Fig. 7(a). Fig. 7(b) is the corresponding [001] projection image including both disordered and  $1/2\{100\}$  ordered structure. As shown in Fig. 1(d), in  $1/2\{100\}$  chemical ordering, the  $\text{Pb}^{2+}$  and  $\text{Ca}^{2+}$  cations are arranged in alternate layers along one of the  $\langle 100 \rangle$  direction, e.g. [010] in Fig. 7(b). Thus the  $1/2\{100\}$  superlattice fringes with spacing of 0.778 nm in HREM (Fig. 7(a)) as well as the superlattice diffraction points in SAD (Fig. 6) exist only in one direction.

#### 4. Discussion

High resolution micrographs have shown apparently that not only  $1/2\{111\}$  superlattice, but also  $1/2\{110\}$  and  $1/2\{100\}$  superlattices come from the chemical ordering of  $\text{Pb}^{2+}$  and  $\text{Ca}^{2+}$  cations aligned in alternate layers along different directions. It seems that they are not the result of electrical ordering due to atomic shuffles. In fact, three different types of chemical ordering can coexist in the same sample and even in the same grain; there are two different chemical

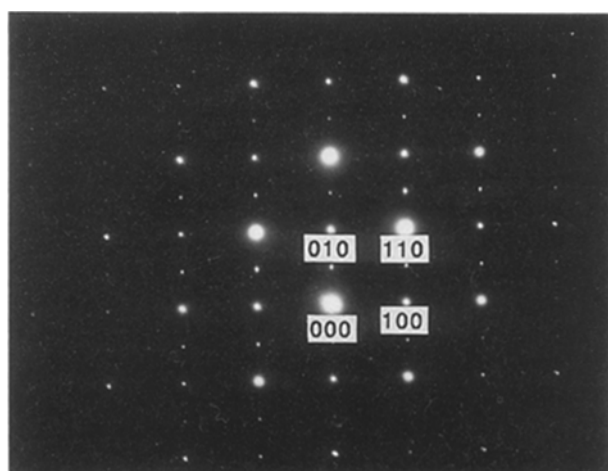


Figure 6 Another [001] zone axis electron diffraction pattern with  $1/2\{100\}$  superlattice reflections.

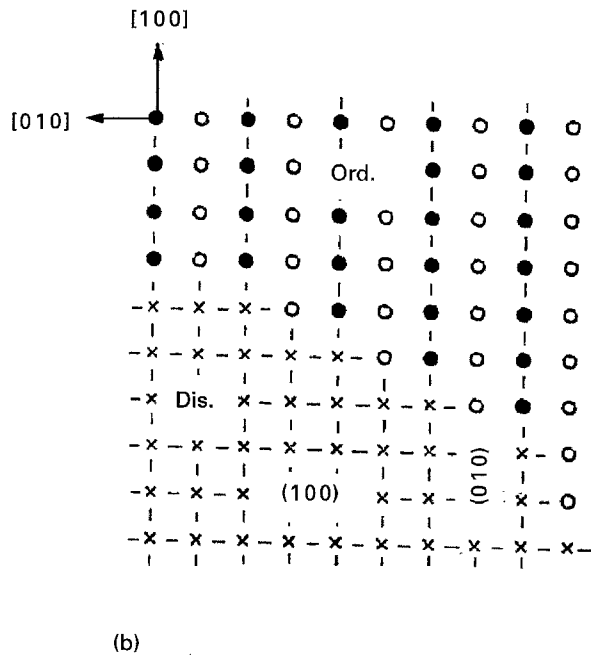
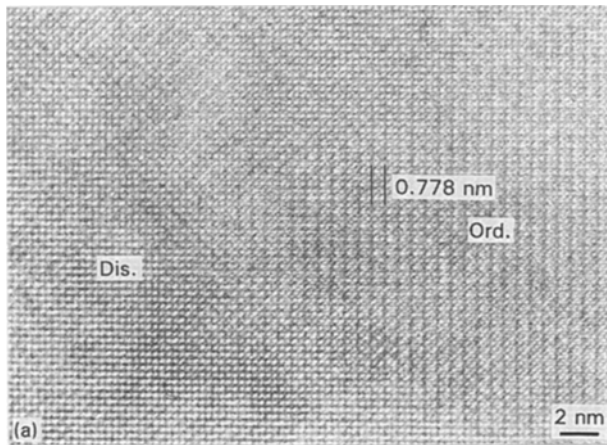


Figure 7 (a) A [001] zone axis HREM image with  $1/2\{100\}$  ordered structure regions. (b) The projection image of  $\text{Pb}^{2+}$  and  $\text{Ca}^{2+}$  cations on (001) plane for both disordered and  $1/2\{100\}$  ordered structure.

orderings (see Fig. 4). These imply that apart from the nearest interaction, the second and the third neighbour interaction also play an important role in the superstructure formation and there is not much energy difference for the three different superstructures [9].

As shown in Fig. 3(a) for  $1/2\{111\}$  ordering, it has been revealed that the unit cell of the ordered region is not just double the disordered ones and somewhat deviated from the cubic structure. It can be noted that the orientation of crystallization in the ordered regions is not fully consistent with the neighbouring disordered ones, causing the formation of a “vernier boundary” (see Fig. 3(b)); the degree of deformation has been exaggerated for clarity. What should be pointed out is that the “vernier boundary” is somewhat similar but not exactly the same as dislocation. A dislocation is normally considered as a line defect while the “vernier boundary” has to be considered as a face imperfection and always appears to be a curved

interface. Furthermore, the boundary between these kinds of ordered and disordered regions is rather irregular with a comparatively broader deformed transition area.

However, for  $1/2\{001\}$  and  $1/2\{110\}$  ordering, although the boundary between the ordered and the disordered regions is irregular, the crystallization orientation of the ordered and disordered regions is consistent and there is no such broad deformed transition area near the boundary as that for  $1/2\{111\}$  ordering.

The ordered and the disordered regions coexist in one grain and basically keep their original crystallization orientation. The size of the ordered and disordered domains are from 2 to 30 nm. The relationship between the ordered and disordered domains and their distribution in lattice level have also been studied in  $(\text{Pb}(\text{Sc}_{0.5}\text{Ta}_{0.5})\text{O}_3)$  [10]. It has been suggested that the nanoscale ordered domains act as natural sites on which to localize the superparaelectric polar cluster, the scale of it being the basis of classification between normal and relaxor ferroelectrics. By using HREM, the fine superstructure in nanoscale has been exposed for  $(\text{Pb}_{0.5}\text{Ca}_{0.5})\text{TiO}_3$ . However, further studies on the relationship between the microstructure and properties of lead–calcium titanate ceramics are being carried out.

## 5. Conclusions

The structural characteristics of ordered  $(\text{Pb}_{0.5}\text{Ca}_{0.5})\text{TiO}_3$  was investigated by using HREM, the results obtained can be summarized as follows:

1. HREM images reveal that there are three types of chemical ordering –  $1/2\{111\}$ ,  $1/2\{110\}$  and  $1/2\{100\}$  coexisting in  $(\text{Pb}_{0.5}\text{Ca}_{0.5})\text{TiO}_3$ .
2. The fine structure of both ordered and disordered domains has been exposed in lattice level, the size of it being 2–30 nm.
3. The unit cell of  $1/2\{111\}$  superstructure is somewhat deviated from ideal cubic structure, causing a special kind of boundary – “vernier boundary” between  $1/2\{111\}$  ordered and disordered regions.
4. The scale and distribution of ordered and disordered domains were considered to be correlated with relaxor or normal ferroelectric properties.

## Acknowledgements

The authors acknowledge the financial support of the Chinese National Science Foundation (No. 59232041) and the help of Mr Q.M. Wang and Mr J.H. Zao in obtaining the HREM images.

## References

1. U. CHINO, *Amer. Ceram. Soc. Bull.* **65** [4] (1986) 647.
2. F. UCHIKOBA and K. SAWAMURA, *Jpn. J. Appl. Phys.* **31** (1992) 3124.
3. F. OSAMU, Y. YOHACHI and H. MITSUO, *Ibid.* **30** [9b] (1994) 2303.

4. C. A. RANDALL, A. S. BHALLA, T. R. SHROUT and L. E. CROSS, *J. Mater. Res.* **5** [4] (1990) 829.
5. XIAOWEN ZHANG, QIANG WANG and BINGLIN GU, *J. Amer. Ceram. Soc.* **74** [11] (1991) 2846.
6. C. RANDALL, D. BARBER, R. WHATMORE and P. GROVES, *Ferroelectrics* **76** (1987) 277.
7. FEI FANG and XIAOWEN ZHANG, *J. Mater. Res.* **10** [7] (1995) 1582.
8. G. KING and E. GOO, *J. Amer. Ceram. Soc.* **71** [6] (1988) 454.
9. BINGLIN GU, JUN NI and XIAOWEN ZHANG, *J. Appl. Phys.* **70** [8] (1991) 4224.
10. L. Y. CAI, X. W. ZHANG and X. R. WANG, *Mater. Lett.* **20** (1994) 169.

*Received 19 October 1994  
and accepted 8 September 1995*